Tellus (1983), *35A*, 149–158

On the mechanics of the deep-water flow in the Bornholm Channel

By PETER LUNDBERG, *Department of Oceanography, University of Gothenburg, Box 4038, S-40040 Gothenburg, Sweden*

(Manuscript received November 25, 1981; in final form April 19, 1982)

ABSTRACT

A model for stationary and longitudinally homogeneous 2-layer rotating canal flow subject to friction is proposed for the deep-water flow in the Bornholm Channel. Using parameter values estimated from the results of a field survey carried out in conjunction with a long-term program for monitoring the inflow of high-saline water to the Baltic, diagnostic calculations for the position of the pycnocline have been performed. The results correspond to an encouraging degree to those observed in nature and indicate the existence of a frictional coupling between the down- and cross-stream pressure gradients in deep-water.

1. Introduction

In the last decade a fair amount of work has been done concerning rotating two-layer canal flow (Whitehead et al., 1974; Gill, 1976; Sambuco and Whitehead, 1976). One of the main aims of this research, inspired by conventional nonrotating hydraulics, has been to elucidate how control is imposed upon the flow by the topographical and rotational constraints. Since the greater part of the above-mentioned work has been orientated towards theoretical analysis and laboratory experiments, it is the hope of the present author that some interest might accrue to field study of the mechanics of the inflow of deep water to the Baltic, a process which with a gross simplification might be described as an instance of two-layer rotating canal flow. The investigation to be reported here has been undertaken in conjunction with a long-term field program for monitoring the Baltic high-saline deep-water inflow conducted by the Department of Oceanography, University of Gothenburg (Petrén and Walin, 1976; Walin, 1977, 1981). During this project, the hydrographical section chosen for detailed study was situated between southern Sweden and the Danish island of Bornholm (Fig. 1) through where, as is generally acknowledged, the entire renewal of the Baltic deep-water takes place. The routine measurements consisted of CTD-stations in addition to current measurements in the high-saline deep-water at 2-m intervals in the vertical at the standard positions A1, A2, A3, A4, C1, C2 and C3 of Fig. 1. Hereby a synoptic image of the inflow situations was obtained which was used for assembling statistically significant averages of the deep-water volume-flux into the Baltic as a function of the salinity as reported by Walin (1981).

On the basis of some of these synoptic surveys, it has recently been suggested that the flow of deep-water is hydraulically controlled at precisely the section under investigation (Rydberg, 1980). In the opinion of the present author, the evidence for this assumption is however quite slender and might instead be interpreted as supporting the view to be advanced in this paper, namely that the flow is frictionally balanced. The nature of this balance can perhaps most easily be illustrated by examining the frictionally-controlled interaction between the longitudinal (in the sense of the overall direction of the flow) and transverse pressure gradients in the deep-water. Here this will be done through a series of diagnostic calculations using an equation governing the position of the interface for stationary

 0280-6495/83/020149-10$02.50/0

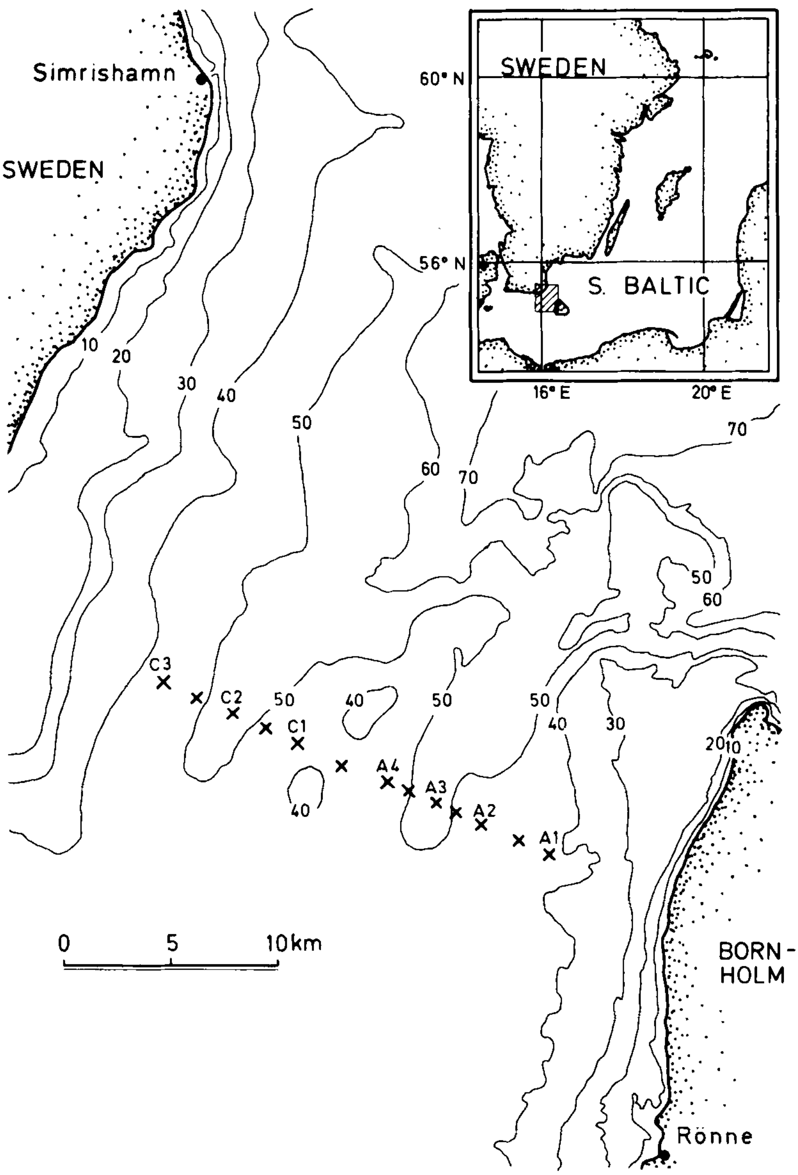

Fig. 1. Map of the Bornholm Channel. The crosses indicate the hydrographic section investigated during the field survey. Depths are in metres.

2-layer rotating canal flow for a prescribed value of the longitudinal pressure gradient in the deep-water. These computations have been undertaken for parameter values of the model adjusted to the conditions observed on one of the surveys of the Bornholm Channel. During this field experiment, however, the distance between adjacent hydrographical stations was halved in comparison with routine procedures. Furthermore the current measurements were taken with more dense spacing than usual and extended to also include the upper layer, all in order to ensure adequate resolution in view of the diagnostic calculations which were to ensue. In addition, a number of computations were undertaken for varying but not unrealistic values of the vertical exchange coefficient and the longitudinal pressure gradient in order to illustrate the dependence of the flow upon these particular parameters.

In Section 2, the ordinary differential equation governing the position of the interface is discussed and a technique for its numerical solution outlined, whereafter Section 3 deals with the results of the field experiments. In Section 4, the results of diagnostic calulations are compared with those of the field study, and furthermore the overall results are subjected to a discussion in view of the approximate nature of the mathematical model.

2. The governing equation

We consider the system shown in Fig. 2 which schematically depicts the constant cross-section of a canal extending in the y-direction. In a rotating reference frame ($\underline{\Omega} = \Omega\hat{z}$), 2 layers of water of densities $\rho - \Delta\rho$ and ρ are separated by an interface at distance $H(x)$ above the bottom, which in turn is situated a distance $B(x)$ above a horizontal reference level. The interface permits diffusion of momentum but not of density and the velocities in the upper and lower layers are $\mathbb{V}_u$ and $\mathbb{V}$ respectively. Under stationary conditions the equation of motion for the lower layer is:

$$\mathbb{V} \cdot \nabla\mathbb{V} + 2\underline{\Omega} \times \mathbb{V} + g\hat{z} = -\frac{1}{\rho}\nabla p + A_H \nabla_H^2 \mathbb{V} + A_V \frac{\partial^2 \mathbb{V}}{\partial z^2}, \tag{1}$$

where p is the pressure and g the acceleration of gravity, whereas A_V and A_H are the vertical and horizontal coefficients of momentum exchange and ∇_H^2 is the horizontal Laplacian. The continuity equation is:

$$\nabla \cdot \mathbb{V} = 0. \tag{2}$$

The velocity must satisfy $\mathbb{V} = 0$ on the solid boundary whereas on the interface:

$$\mathbb{V} = \mathbb{V}_u, \qquad \frac{\partial \mathbb{V}}{\partial n} = -\frac{\partial \mathbb{V}_u}{\partial n}, \qquad \mathbb{V} \cdot \mathbb{n} = 0, \tag{3}$$

where $\partial/\partial n$ is the derivative along the normal $\mathbb{n}$ directed inwards with respect to the surface on which $\partial/\partial n$ is evaluated, and where it has been assumed that the vertical exchange coefficient is equal on both sides of the interface. A similar set of equations and boundary conditions can be formulated for the flow in the upper layer. Note that in this latter case the boundary conditions on the free surface can include the effects of a wind-stress, a possibility which however will be neglected in the present treatment of the problem where the forcing is due to a prescribed constant downstream pressure gradient in the deep-water slightly modified by a pressure field associated with the free surface of the upper layer. In principle, the 2 coupled sets of differential equations should now be solved simultaneously, but since we are interested in the deep-water flow we focus our attention on equations (1), (2) and (3). The problem will be treated as longitudinally homogeneous and thus all derivatives in the y-direction disappear with the exception of $\partial p/\partial y$ = const., which we prescribe. This longitudinal pressure gradient can be divided into a barotropic, $\partial p_{BT}/\partial y$, and a baroclinic part, $\partial p_{BC}/\partial y$, associated with the inclination of the free surface and the interface, respectively. We moreover prescribe a transverse barotropic pressure gradient $\partial p_{BT}(x)/\partial x$ which is allowed to vary with x. This is in contrast to the longitudinal pressure gradients which must be constant in the cross-stream direction so as not to violate the assumed

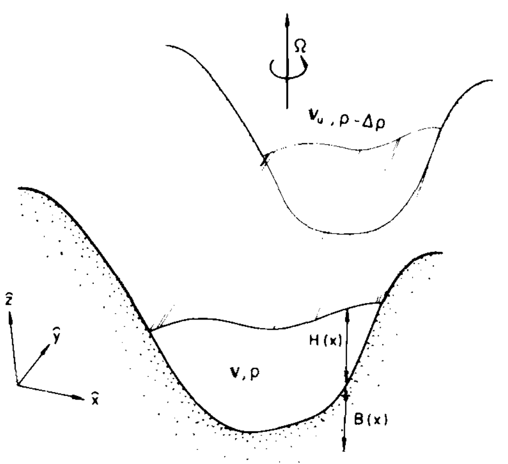

Fig. 2. Sketch of the idealized, lengthwise homogeneous and two-layer stratified canal.

two-dimensionality of the problem. Here it is of great importance to note that the barotropic pressure gradients cannot be prescribed in an arbitrary manner, since they constitute the solutions to the stationary, longitudinally homogeneous upper-layer problem. As we saw above, this problem should actually be solved simultaneously with the one governing the behaviour of the lower layer, but in deriving the equation for the position of the interface we will limit ourselves to regarding the prescribed barotropic pressure gradients as being consistent with a stationary solution for the upper layer. When using the model for diagnostic purposes, this assumption must of course be checked carefully *a posteriori*, a topic we shall return to when applying the theory to the results of the field experiment.

Following Welander (1968) an equation governing the position of the interface under stationary conditions can now be obtained by integrating the continuity equation (3) vertically through the lower layer. Together with use of the boundary conditions this yields:

$$\int_{B(x)}^{B(x)+H(x)} u \, \mathrm{d}z = C. \tag{4}$$

Since the walls of the canal are impermeable, the constant C is equal to zero and thus the stationarity condition implies that there be no vertically integrated cross-stream transport in the lower layer. The cross-stream velocity $u(x,z)$ must now be determined. Formally this is accomplished by a nondimensionalization of the governing equations and by noting that under conditions of small Ekman and Rossby numbers the velocity field $\mathbb{V}$ can be decomposed into a geostrophic interior:

$$u^{\mathrm{I}} = -\frac{1}{2\Omega\rho}\left(\frac{\partial p_{\mathrm{BT}}}{\partial y} + \frac{\partial p_{\mathrm{BC}}}{\partial y}\right) \tag{5}$$

$$v^{\mathrm{I}} = g\frac{\Delta\rho}{\rho}\frac{1}{2\Omega}\frac{\partial}{\partial x}(H(x) + B(x)) + \frac{1}{2\Omega\rho}\frac{\partial p_{\mathrm{BT}}}{\partial x} \tag{6}$$

and frictionally balanced boundary layers. Under the assumption of a small aspect ratio of the canal topography, the transport (m_x, m_y) of the bottom Ekman layer is:

$$m_x = \frac{1}{2}\sqrt{\frac{A_{\mathrm{V}}}{\Omega}}(-u^{\mathrm{I}} - v^{\mathrm{I}}), \tag{7}$$

$$m_y = \frac{1}{2}\sqrt{\frac{A_{\mathrm{V}}}{\Omega}}(u^{\mathrm{I}} - v^{\mathrm{I}}), \tag{8}$$

whereas the transport (m_x^i, m_y^i) of the Ekman layer adjacent to the interface is:

$$m_x^i = \frac{1}{4}\sqrt{\frac{A_{\mathrm{V}}^i}{\Omega}}[-(u^{\mathrm{I}} - u_{\mathrm{u}}^{\mathrm{I}}) - (v^{\mathrm{I}} - v_{\mathrm{u}}^{\mathrm{I}})] \tag{9}$$

$$m_y^i = \frac{1}{4}\sqrt{\frac{A_{\mathrm{V}}^i}{\Omega}}[(u^{\mathrm{I}} - u_{\mathrm{u}}^{\mathrm{I}}) - (v^{\mathrm{I}} - v_{\mathrm{u}}^{\mathrm{I}})], \tag{10}$$

where A_{V}^i is the vertical exchange coefficient in the region of the interface and $u_{\mathrm{u}}^{\mathrm{I}}$, $v_{\mathrm{u}}^{\mathrm{I}}$ are the geostrophically balanced interior velocities in the upper layer due to the prescribed barotropic pressure gradients. By inserting eqs. (5), (7) and (9) in (4), a first-order differential equation for the position $H(x)$ of the interface is obtained:

$$\begin{aligned}
&\left(\frac{1}{2}\sqrt{\frac{A_{\mathrm{V}}}{\Omega}} + \frac{1}{4}\sqrt{\frac{A_{\mathrm{V}}^i}{\Omega}}\right)\frac{g}{2\Omega}\frac{\Delta\rho}{\rho}\frac{\partial H(x)}{\partial x} \\
&= -\frac{1}{2\Omega\rho}\left(\frac{\partial p_{\mathrm{BT}}}{\partial y} + \frac{\partial p_{\mathrm{BC}}}{\partial y}\right)H(x) \\
&+ \left(\frac{1}{2}\sqrt{\frac{A_{\mathrm{V}}}{\Omega}} + \frac{1}{4}\sqrt{\frac{A_{\mathrm{V}}^i}{\Omega}}\right)\frac{1}{2\Omega\rho}\frac{\partial p_{\mathrm{BC}}}{\partial y} \\
&- \frac{1}{2}\sqrt{\frac{A_{\mathrm{V}}}{\Omega}}\cdot\frac{1}{2\Omega\rho}\left(\frac{\partial p_{\mathrm{BT}}}{\partial x} - \frac{\partial p_{\mathrm{BT}}}{\partial y}\right) \\
&- \left(\frac{1}{2}\sqrt{\frac{A_{\mathrm{V}}}{\Omega}} + \frac{1}{4}\sqrt{\frac{A_{\mathrm{V}}^i}{\Omega}}\right)\frac{g}{2\Omega}\frac{\Delta\rho}{\rho}\frac{\partial B(x)}{\partial x},
\end{aligned} \tag{11}$$

where $u^{\mathrm{I}} - u_{\mathrm{u}}^{\mathrm{I}}$ and $v^{\mathrm{I}} - v_{\mathrm{u}}^{\mathrm{I}}$ to a high degree of accuracy have been represented as the baroclinic components of the geostrophic flow in the lower layer. From eqs. (6), (8) and (10), a horizontal integration yields Q, the total downstream transport in the lower layer:

$$Q = \int_{x_s}^{x_f} (v^{\mathrm{I}}(x)\,H(x) + m_y + m_y^i)\,\mathrm{d}x, \tag{12}$$

where x_s and x_f are the points of intersection between the bottom and the interface. For a fixed value of Q, eq. (11) uniquely determines the position of the interface since there is a one-to-one correspondence between x_s and $Q(x_s)$. Consequently an initial-value problem for the position of the interface $H(x)$ can be posed with $H(x_s) = H_s$. Since the model cannot cope with situations where the height of the interface above the bottom is not of the same order as or larger than the sum of the boundary-layer thicknesses we take this intitial value to be:

$$H_s = \frac{1}{2}\sqrt{\frac{A_V}{\Omega}} + \frac{1}{4}\sqrt{\frac{A_V^i}{\Omega}}. \tag{13}$$

We note that even though the inclusion of a spatially dependent barotropic cross-steam pressure gradient represents a deviation from established practice, the solution to the problem as outlined here is consistent with the channel approximation (Simons, 1980). Since the initial-value problem has been formulated for an arbitrary bottom profile it can in general only be solved by numerical integration. In the practical computations, a 4-level Runge-Kutta scheme was used to generate a manifold of solutions $|H(x), Q(x_s)|$ from which the one with a transport Q corresponding to the case under investigation could be selected; hence the term diagnostic calculation. The solutions were computed under the restrictions that $dB/dx|_{x=x_s} < 0$ and that the interface should not intersect the free surface. In each case $H(x_i) = H_s$ provided a suitable criterion for terminating the integration. Finally we note that experience has revealed that the numerical scheme imposes certain regularity constraints on the coefficients of the governing equation. Not only must these be continuous, but the same must hold true for their derivatives so as not to generate spurious effects in the numerical solution.

3. The field experiment

On August 11, 1976 an extensive hydrographic survey of the Bornholm Channel was undertaken. As shown in Fig. 1, this constriction between southernmost Sweden and the Danish island of Bornholm has an approximate width of 30 km and a threshold depth of around 50 m. It is generally assumed that the total deep-water renewal of the Baltic takes place through this channel. Possibly an influx of deep-water also through the slightly shallower canal adjacent to Adlergrund south-west of Bornholm could occur under exceptional circumstances, but this is however conjecture since it has never been observed during the extensive hydrographic field program referred to in the introduction. When judging the relevance of the 2-dimensional model outlined in Section 2 for the deep-water flow through the Bornholm Channel, it is immediately evident from the isobaths of Fig. 1 that the channel is not perfectly longitudinally homogeneous in character. Neither does in fact nature conform to the proposed 2-layer idealization. Large vertical density gradients are encountered, which is not surprising since the water mass typically consists of a brackish surface layer of largely Baltic origin above the high-saline deep water emanating from the Kattegatt-Skagerrak area, but the density stratification is not discontinuous and the pycnocline certainly permits vertical exchange of density as well as momentum. Discouraging as this may seem, it is however to be kept in mind that our aim is to investigate the gross features of the deep-water flow. Thus it is not unreasonable to hope that even a model which is only accurate to lowest order may provide some useful insights.

The survey consisted of hydrographic stations using a continuously recording CTD-instrument at the positions indicated by crosses in Fig. 1. Moreover at stations A1, A2, A3, A4, C1, C2 and C3, current measurements were made using gelatine pendulum current meters. These were deployed over the entire water column with the exception of the immediate subsurface layer where wave action would have rendered them useless. Typical spacing in the vertical ranged from $\frac{1}{2}$ – 1 m in the high-saline deep-water to 5 m in the free water mass well above the pycnocline. In addition to this section a number of other CTD-stations were taken along the channel to determine the downstream slope of the pycnocline.

The hydrographical conditions encountered were rather unusual as is evident from Fig. 3. This comprehensive T-S diagram incorporates the results at depth intervals of 1 m for the entire cross section of the channel. In addition to the readily identifiable "Baltic" and "Skagerrak" water masses, a third type of water is present, characterized by low temperature and low salinity. The origin of this is obscure, the most likely explanation being that it results from the wintertime convection of Baltic surface water. Note that in view of the proposed 2-layer idealization of the flow, the presence of 3 distinct water masses could prove troublesome. However, in Fig. 4 the isotherms of the deeper part of the hydrographic section are graphed. The diagram shows the complicated thermal structure present in the southern part of the section, but it also reveals that the cold-water mass

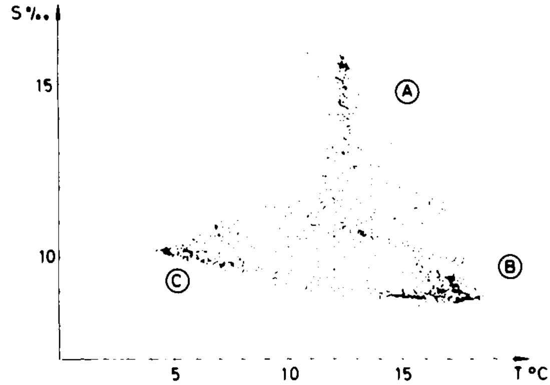

Fig. 3. Temperature/salinity (T-S) diagram illustrating overall conditions in the Bornholm Channel on August 11, 1976. Three types of water can be distinguished. A: Cold high-saline Skagerrak water. B: Warm, brackish Baltic surface water. C: Very cold, brackish Baltic winter water.

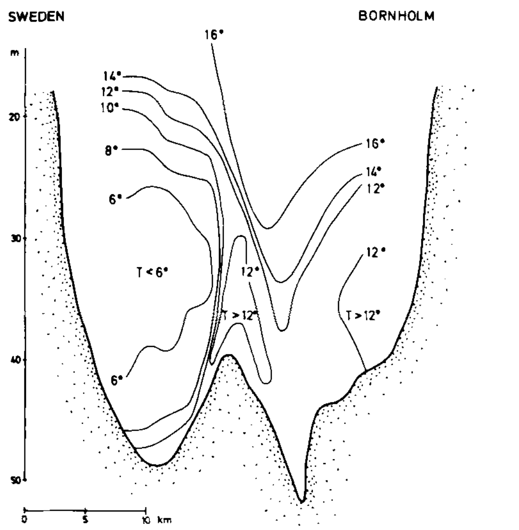

Fig. 4. Isothermals in the deeper regions of the cross section from Bornholm to Sweden. The vertical scale shows the distance from the free surface.

is confined to an intermediate region north of a small submarine ridge. South of this ridge the conditions are more favourable for an application of our model and in what follows we thus limit ourselves to a study of this region. In order to provide guidelines for the determination of the respective densities of the idealized two-layer situation to be used in the forthcoming computations, a frequency distribution of σ_t as observed in the southern part of the section is presented in Fig. 5. The skewness of the distribution is due to all observations having been given the same weight. This allows Baltic water, which occupies the by far largest part of the cross-section area, to dominate. However, Skagerrak water ($\sigma_t > 10$) is seen to constitute a distinct part of the distribution. A choice of the isopycnal $\sigma_t = 10$ as the idealized interface between the upper and lower water masses resulted, after an averaging procedure, in $\rho = 1011.108$ kg m^{-3} and $\Delta\rho = 4.431$ kg m^{-3}.

In the southern part of the section, current measurements were made at 4 stations: A1, A2, A3, and A4. Table 1 shows depth-averaged values of the observed cross- and down-stream velocity components in the interior of the upper layer.

Under the assumption of a geostrophically balanced interior flow, these velocities are proportional to the barotropic pressure gradients to be

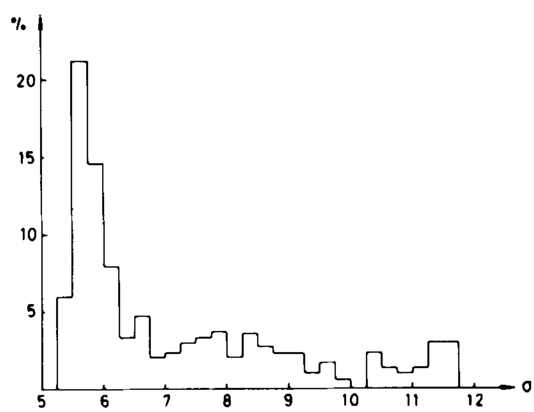

Fig. 5. Frequency distribution of σ_t-observations at 1 m intervals from surface to bottom in the southern part of the hydrographic section shown in Fig. 1.

Table 1. *Vertically averaged current velocities in the upper layer*

Position	A1	A2	A3	A4
u_u (10^{-2} m s^{-1})	0.5	5.4	−0.2	0.4
v_u (10^{-2} m s^{-1})	11.1	4.3	3.3	−8.5

prescribed in the numerical model. Even though the cross-stream velocities on the average are an order of magnitude smaller than their downstream counterparts, it is evident that the cross-stream variation of u_u violates the assumed longitudinal homogeneity of the flow. A cursory examination of the observed barotropic velocities furthermore reveals that they are most likely not compatible with stationary conditions in the upper layer. However, in view of the fact that the interior flow in the upper layer is predominantly directed along the channel and thus at least grossly conforms to our requirement of two-dimensionality, an average value of the cross-stream velocity $\bar{u}_u = 1.5 \times 10^{-2}$ m s^{-1} was used in the diagnostic calculations. This average has been weighted with regard to the differing horizontal spacing of stations A1 to A4. In order to provide adequate continuous data for the numerical calculations, a cubic spline was fitted to the observations of the longshore velocities. By examining the measured velocity profiles close to the bottom it was seen that the shear layers had a thickness of around 2 m. Since the boundary-layer thickness is of order $(A_V/\Omega)^{1/2}$, a crude estimate yielded $A_V \approx 3 \times 10^{-4}$ m^2 s^{-1}. The vertical exchange coefficient associated with the interface was assumed to be $A_V^i = \frac{1}{4}A_V$. Even though this latter appraisal must be judged as physically not unreasonable, lack of experimental data has precluded any attempt to justify this estimate empirically.

In order to close the diagnostic problem, the baroclinic pressure gradient due to the downstream slope of the interface was determined through a series of hydrographic stations along the channel. Note that direct measurement of this quantity is no easy task, since the interface also displays a strong cross-channel inclination, which even in the idealized case of a longitudinally homogeneous canal would make small lateral deviations in the positioning of the hydrographic stations result in large errors. As we have seen, the Bornholm channel is topographically irregular and during the survey the hydrographic conditions were further complicated by the presence of the cold and low-saline water-mass discussed above. Nevertheless an estimate, based on the long-channel measurements and tempered by knowledge of the overall conditions in the southern Baltic, indicated that $dp_{BC}/dy \approx 4.35 \times 10^{-3}$ kg m^{-2} s^{-2}, equivalent to a lengthwise slope of the interface of 10^{-4}.

4. Results and discussion

Using the parameter estimates of Section 3, a number of solutions to eq. (11) have been computed for increasing values of x_s, the starting point. Since the synoptic hydrographic survey included densely spaced current measurements in the deepwater, the total downstream transport below the σ_t = 10 isopycnal was known to be around 7000 m^3 s^{-1}. Thus the numerical solutions with long-channel transports in the lower layer $Q(x_s)$ most closely equalling the one observed could be selected for inspection. (Since a discretization of the x-coordinate was used for numerical purposes, it was not always possible to obtain a single-valued best approximation.) Fig. 6 shows the southern part of the hydrographic section. The computed position of the interface is shown by a shaded band where the upper delimitation is associated with $Q = 7370$ m^3 s^{-1} whereas for the lower $Q = 6590$ m^3 s^{-1}. The field measurements of the $\sigma_t = 10$ isopycnal are represented by dots interconnected by a cubic spline and shown within their observational margin of error (hatched). A comparison between prediction and observation indicates that the diagnostic

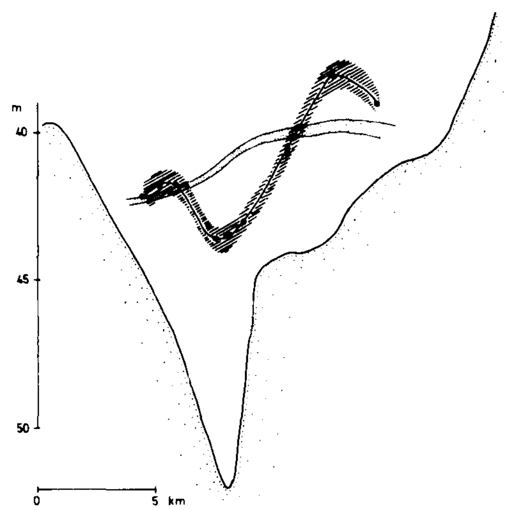

Fig. 6. This graph limits itself to the southern part of the hydrographic section of Fig. 1. The shaded zone indicates the numerically predicted position of the interface. The discrete points interconnected by a cubic spline show the actually measured position of the pycnocline within its margin of error (hatched).

solution is not too widely off the mark even though the accuracy is not overwhelming. However, in view of the approximate nature of the model, it would indeed have been surprising had it yielded a perfect fit.

Once the position of the interface and the associated downstream velocity in the lower layer have been determined, the assumption of a stationary flow in the upper layer can be checked. When neglecting the possibility of a surface Ekman layer, the vertically integrated cross-stream transport in the upper layer is found to be:

$$C_u = v_u^I(x)(T - H(x) - B(x)) + \frac{1}{4}\sqrt{\frac{A_V^I}{\Omega}}\,[(u^I - u_u^I) + (v^I - v_u^I)]. \tag{14}$$

Here $z = T$ is the position of the free surface; in the Bornholm Channel $T = 52$ m. We choose to study the case of $Q = 7370$ m^3 s^{-1}. Table 2 shows the value of C_u at some representative cross-stream positions including the delimiting points x_s and x_f of the region where eq. (14) is valid.

In a case like this, when the section under investigation has no lateral walls, a constant cross-stream transport C_u is in principle a sufficient criterion for stationarity. Nevertheless, from Table 2 it is clear that the sole possibility of obtaining stationary conditions in the upper layer lies in extending the analysis to also incorporate a wind-induced surface Ekman layer with varying cross-stream transport. Unfortunately no observations of the wind were made during the field survey. Thus we will have to assume, post festum, that the wind conditions were such that stationary conditions could prevail. In view of previous results (Petrén and Walin, 1976), which demonstrate a high degree of correlation between the hydrographic conditions encountered in the Bornholm Channel on consecutive days, this assumption is not unreasonable. In order to judge the influence of possibly erroneously prescribed barotropic pressure gradients, diagnostic calculations have also been performed assuming no motion in the upper layer and for consistency also neglecting the effects of interfacial stresses. Fig. 7 shows the computed positions of the interface for the 2 cases. The solid line corresponds to the case of barotropic forcing ($Q = 7370$ m^3 s^{-1}) whereas the dashed line indicates the result for a passive upper layer ($Q = 6970$ m^3 s^{-1}). From the graph it is evident that for the range of barotropic motion prescribed here, the position of the interface is dominated by the dynamics of the lower layer. This would tend to reinforce confidence in the proposed model since the magnitudes of the barotropic forcing used in the computations above are representative of the upper-layer velocities usually encountered in the Bornholm Channel.

The diagnostic calculations are dependent upon a number of parameters, the most difficult one of which to estimate precisely was the vertical exchange coefficient. Even though the estimate $A_v = 3 \times 10^{-4}$ m^2 s^{-1} most likely is correct to order of magnitude, it seems doubtful whether too much faith should be placed in it. In order to judge the sensitivity of the model to this parameter, a number

Table 2. *Vertically integrated cross-stream transport in the upper layer*

Position	x_s	A3	A2	A1	x_f
C_u (m^2 s^{-1})	0.66	0.71	0.63	0.59	0.58

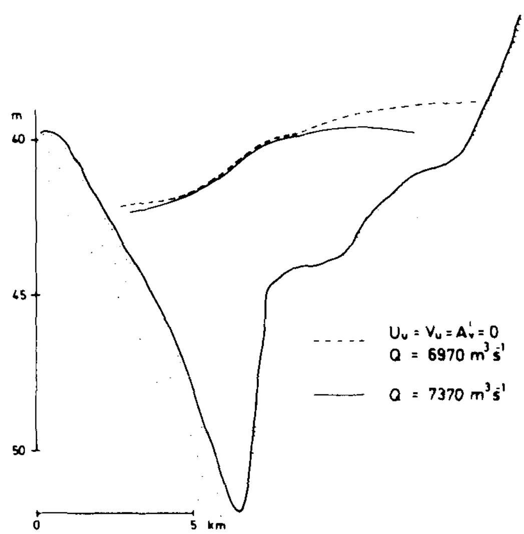

Fig. 7. Computed positions of the interface for the case of barotropic forcing (solid line) and for a passive upper layer (dashed line).

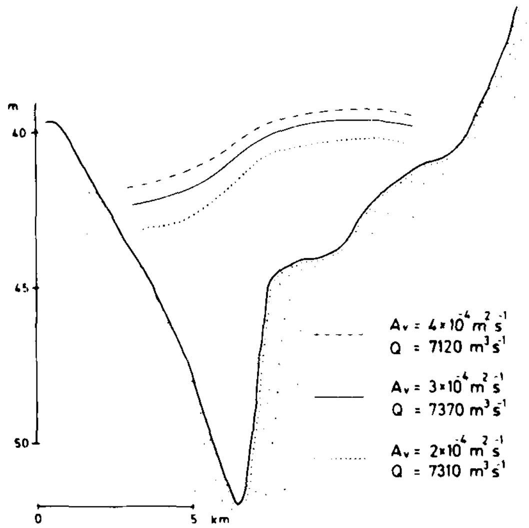

Fig. 8. Numerical predictions of the position of the interface for different values of the vertical exchange coefficient.

of calculations have been undertaken with A_V assuming a physically plausible range of values in the neighbourhood of the original estimate. In Fig. 8 the results are shown for $A_V = 2 \times 10^{-4}$ (dotted line), $A_V = 3 \times 10^{-4}$ (solid line) and $A_V = 4 \times 10^{-4}$ $m^2\ s^{-1}$ (dashed line). These diagnostic solutions all have downstream transports in the lower layer of around 7000 $m^3\ s^{-1}$ and are subject to the experimentally determined barotropic and baroclinic forcing. It is recognized that under stationary conditions, smaller values of A_V require larger downstream baroclinic velocities in order to compensate the diminished transports of the Ekman layers. Consequently a lower level as well as a steepening of the interface should result and this is borne out by the figure. The same effects were encountered when A_V^i, which in a somewhat arbitrary manner had been taken to be $\frac{1}{4}A_V$, was allowed to vary in magnitude from 0 to A_V while retaining the original estimates of all other parameters. In this case however, the effects were less pronounced than those demonstrated by Fig. 8, since the boundary-layer transports associated with the interface are smaller than those at a solid boundary. Thus it is recognized that even though the model is sensitive to the magnitudes of the vertical exchange coefficients, it yields qualitatively acceptable results for values of these parameters within a physically reasonable range. We furthermore note that during the course of a typical year, the downstream slope of the interface in the Bornholm Channel may vary from 5×10^{-5} to 3×10^{-4}. From a series of diagnostic calculations with prescribed downstream pressure gradients in this range, it was found that the model yielded results which did not contradict the field observations by Petrén and Walin (1976). These computations were undertaken for a passive upper layer and assuming homothermal conditions with salinities of 8 and 15 parts per thousand in the upper and lower layers respectively, while $A_V = 3 \times 10^{-4}$ $m^2\ s^{-1}$. Even though the results in themselves lack interest, corresponding as they do to strongly idealized cases, we note that they failed to reveal any inconsistencies in the model.

When judging the results reported above it must be kept in mind that these are based upon a number of independent experimental estimates of the parameters governing the flow and that in no case have any parameters been adjusted to ensure good correspondence between predictions and observations. Since an auxiliary condition on the total down-stream transport in the lower layer was necessary to close the problem, the model is purely diagnostic in character and consequently lacks any predictive value. Nevertheless the results indicate that a frictionally controlled interaction between the down- and cross-stream pressure gradients in deep-water is compatible with observed features of the flow in the Bornholm channel. It has moreover been demonstrated that the model is comparatively insensitive to moderate changes of the experimentally determined parameters, which may serve as an indication that it is accurate at least to lowest order.

To conclude we might note the important rôle that the magnitude of the downstream pressure gradient in the lower layer plays in determining the position of the pycnocline separating the brackish surface water from the dense, high-saline deep-water. In view of the fact that the conditions observed during the reported field survey in no way were atypical of those usually encountered in the channel (Petrén and Walin, 1976), this certainly indicates that friction must be taken into consideration when analyzing the deep-water flow through the Bornholm Channel.

5. Acknowledgements

The author wishes to thank Prof. Gösta Walin for valuable discussions and furthermore acknowledges the skill and perseverance displayed by the crew and officers of N/O *Svanic* during the field experiment. Kristina Hansson and Agneta Hilding were most helpful in the technical preparation of this manuscript.

REFERENCES

Gill, A. E. 1976. Adjustment under gravity in a rotating channel. *J. Fluid Mech. 77*, 603–621.

Petrén, O. and Walin, G. 1976. Some observations of the deep flow in the Bornholm Strait during the period June 1973—December 1974. *Tellus 28*, 74–87.

Rydberg, L. 1980. Rotating hydraulics in deep-water channel flow. *Tellus 32*, 77–89.

Sambuco, E. and Whitehead, J. A. 1976. Hydraulic control by a wide weir in a rotating fluid. *J. Fluid Mech. 73*, 521–528.

Simons, T. J. 1980. Circulation models of lakes and inland seas. *Can. Bull. Fish. Aquat. Sci. 203*: 146 p.

Walin, G. 1977. A theoretical framework for the description of estuaries. *Tellus 29*, 128–136.

Walin, G. 1981. On the deep water flow into the Baltic. *Geophysica 17*, 75–93.

Welander, P. 1968. Wind-driven circulation in one- and two-layer oceans of variable depth. *Tellus 20*, 1–15.

Whitehead, J. A., Leetmaa, A. and Knox, R. A. 1974. Rotating hydraulics of strait and sill flows. *Geophys. Fluid Dyn. 6*, 101–125.